Applied Catalysis B: Environmental 119–120 (2012) 132–138

Contents lists available at SciVerse ScienceDirect

Applied Catalysis B: Environmental

journal homepage: www.elsevier.com/locate/apcatb

Modelling photo-Fenton process for organic matter mineralization, hydrogen peroxide consumption and dissolved oxygen evolution

A. Cabrera Reina[a,b], L. Santos-Juanes Jordá[a,b], J.L. García Sánchez[a,b], J.L. Casas López[a,b], J.A. Sánchez Pérez[a,b,*]

[a] Department of Chemical Engineering, University of Almería, 04120 Almería, Spain
[b] CIESOL, Joint Centre of the University of Almería-CIEMAT, 04120 Almería, Spain

ARTICLE INFO

Article history:
Received 29 December 2011
Received in revised form 19 February 2012
Accepted 21 February 2012
Available online 5 March 2012

Keywords:
Photo-Fenton kinetics
Dissolved oxygen
Paracetamol
Photocatalysis

ABSTRACT

A kinetics model with lumped components and TOC fractionation is proposed to track paracetamol degradation, as a model pollutant, using the photo-Fenton process. The proposed structure shows acceptable predictive capabilities regarding hydrogen peroxide consumption, TOC mineralization and dissolved oxygen evolution. The number of model parameters is considered assumable in calibrating other pollutants and degradation mixtures when applying this technology. This study covers a pollutant load range between 4 and 25 mM of TOC. The Fe^{2+} initial load varied between 0.089 and 0.44 mM whilst the initial H_2O_2 concentration tested ranged from 9 mM to 45 mM. The influence of light intensity was considered explicitly within the model whilst temperature and pH conditions were held constant. The fixed structure model, containing 9 kinetic parameters and 3 stoichiometric coefficients, was later applied to a pollutant mixture with a successful prediction of hydrogen peroxide and TOC profiles.

1. Introduction

Pharmaceuticals and personal care products belong to the emergent contaminant category for wastewater. They are spreading increasingly in the environment yet are difficult to treat using conventional technologies. Advanced oxidation processes (AOPs) have evolved as an efficient alternative for dealing with the degradation of these compounds, prompting considerable attention in the development and implementation of these technologies as final on-site treatments (for industrial wastewater) or as a coupling treatment in activated sludge plant operations (for urban wastewater) [1]. Among these advanced oxidation processes—ozonation, heterogeneous photocatalysis (TiO_2/UV) and Fenton-like processes account for almost 75% of the reported works in this field [2].

No definitive evidence on the superior effectiveness of any one of the above-mentioned technologies has been reported and new features are still under development, especially in combination with heterogeneous Fenton [3]. However, the photo-Fenton process has shown the potential for complete pollutant mineralization providing optimal operation conditions. These imply that hydroxyl radical generation is maximized, whilst providing efficient reaction paths to oxidize organic matter. Photo-Fenton has been tested in mixtures of industrial wastewater, containing COD up to 7000 mg O_2/L, and showed competitive performance with other AOPs [4]. Several aspects of the photo-Fenton process have been studied in recent years. Operational conditions, interferences, reactant dosage, reaction pathways, process economics, etc. are common targets of these studies [5–7]. With regard to kinetics modelling, extensive research can be found in the literature on ozonation and TiO_2 photocatalysis [8,9]. However, there are only comprehensive studies on the photo-Fenton mechanism from the early research carried out on these technologies [10,11]. A considerable number of intermediate radical species, with a similar number of reactions between them, are reported in those papers. In fact, all the reactive species generated during photo-Fenton are still under discussion [12].

Additionally, viability of this advanced oxidation technology is based on enhancement using sunlight. Therefore radiation level, wavelength range and distribution of light inside reactors are also considered to complete the designs. However, the kinetic aspects are not yet fully understood, not for lack of knowledge regarding the elementary reactions and equilibrium steps involved, but because the great interrelation and coupling phenomena appeared when some organics were added to the Fenton reactants.

Two main approaches are chosen in a literature survey on photo-Fenton kinetics: one developing a full description of the process using information from individual reaction (elementary steps) and knowledge of the intermediate composition mixtures. These works follow the setup proposed by Kang et al. [13], where three main

* Corresponding author at: Department of Chemical Engineering, University of Almería, 04120 Almería, Spain. Tel.: +34 950015314.
E-mail address: jsanchez@ual.es (J.A. Sánchez Pérez).

0926-3373/$ – see front matter © 2012 Elsevier B.V. All rights reserved.
doi:10.1016/j.apcatb.2012.02.021

group of reactions are considered (an inorganic chemistry core, the intermediate and parent compound with the inorganic reactants and the interactions between Fe and intermediates). The other alternatives relay on a completely empirical view of the process and use the response surface platform for regression models [14]. Papers using neural networks have been tried as well [15]. Most of the cases these works tracked the oxidation of the parent compound, the hydrogen peroxide consumption and the TOC evolution. The papers by Kusic et al. [14] and Ortiz de la Plata et al. [15] are good exponents of the first principles approach, with 50 and 21 reaction steps, respectively. In the empirical approach the work of Pérez-Moya et al. [16] is a representative example of regression models coupled with design of experiments techniques. These authors and coworkers also explore the first principles approach [17]. However, the pseudo-first-order model is the most common kinetic description, sufficient in explaining parent compound decay or the TOC profiles with a relatively successful fit.

An even more sophisticated modelling environment based on computational fluid dynamic methods has been tested for the integrated design of photoreactor devices [18,19]. In this case, other AOPs were experimented on, with the same core of inorganic reactions. The works of Alpert et al. and Mohajerani et al. apply these techniques and give acceptable predictions for TOC evolution [18,19]. However, the kinetics module has less predictive capabilities than the detailed ones discussed above, due to the nature by which the software handles this information, usually as a user-input equation.

Many other models are being developed from simple mixtures or key compounds, offering great predictive capability with respect to contamination but with either unsuitable or no information concerning O_2 evolution. This is an easily measurable variable with a rapid dynamic and this characteristic acts as key information for tracking and controlling systems based on this particular AOP [20]. This is the main reason for developing and validating a dynamic model with sufficient dissolved oxygen representation capabilities. Some AOPs have been applied to remove paracetamol from aqueous solutions in order to determine reaction mechanisms or degradation pathways, the effect of different catalysts, degradation rates and pH effects [21–25]. Nonetheless, as far as we know, information about an oxidative photo-Fenton model for paracetamol-contaminated water, including oxygen profiles, is not available.

In the present study, the use of simplified photo-Fenton process reactions is proposed to create a model able to simulate TOC, hydrogen peroxide and oxygen evolution. The model covers the following ranges: UV irradiance (13–46 W m^{-2}); iron concentration (0.09–0.45 mM); hydrogen peroxide concentration (9–45 mM) and TOC concentration (4–25 mM). In particular, the model must track the O_2 profile evolved, which is a trusted indicator for the efficient use of the intermediate radicals formed within the photo-Fenton treatment. With this purpose in mind, paracetamol aqueous solutions have been used as the polluted water model.

2. Modelling

In this work, the photo-Fenton oxidation process is represented by four main groups of reactions: the photo-Fenton cycle itself; the oxygen generation/consumption as a result of the reactions taking place; the organic matter oxidation as well as the intermediate formation and final mineralization which complete the contaminant treatment.

The proposed model assumes nine processes and eight states—these being the two ferric species (Fe^{2+} and Fe^{3+}); hydrogen peroxide, H_2O_2; the radicals formed from peroxide (whatever their form), R; the dissolved oxygen, DO; and three states

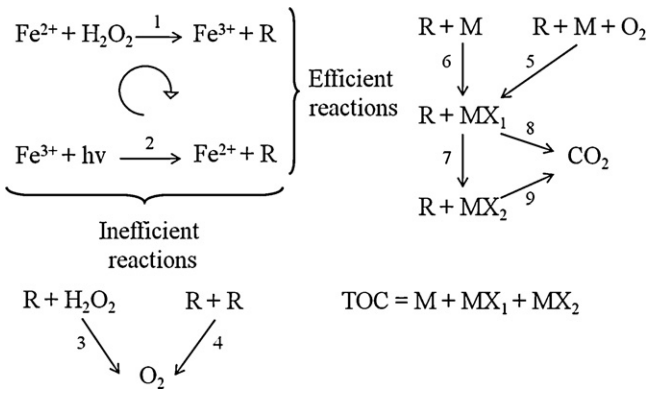

Fig. 1. Proposed reaction scheme.

accounting for the organic matter – two kinds of partially oxidized organics plus the parent compound present at the beginning of the reaction – named as MX_1, MX_2, and M, respectively. These are responsible for the TOC measured. Once the photo-Fenton is initiated, the organic carbon measured is the mass balance of carbon constituent species: unreacted organic carbon, partially oxidized organic material and inert species which have long mineralization times or are non-mineralizable. Note that this last component is not included in the model as a state and should evolve from the model once it is calibrated. The total reaction scheme and the proposed kinetic expressions are presented in Fig. 1 and Table 1, respectively. Note that available light has been considered as another variable in the kinetics, as it is a necessary factor in the process and the photo-Fenton cycle is represented by the minimum possible steps, so as to behave catalytically on the iron species (reactions (1) and (2)).

An intermediate oxidized compound is assumed to be present before any CO_2 is released from the process. In the proposed scheme we have assumed consumption of radicals in all CO_2-releasing steps. The radicals formed in the first two reactions may have a useful pathway, reacting with the organic matter; or may be lost in inefficient reactions with hydrogen peroxide; or lie between them, leading to O_2 generation, which is reflected as a DO increase (reactions (3) and (4)). The remaining reactions are related to the oxidation or intermediate formation ((5)–(7)) and mineralization of the organics ((8) and (9)). Note that direct oxygen consumption is also considered in the first intermediate formation (the Dorfman mechanism) as reflected in the corresponding kinetic expression.

The dynamic model of the photo-Fenton degradation process is based on mass balances for a batch operation mode of the relevant components in the model, as shown in Table 2. The overall gas–liquid mass transfer coefficient for O_2 was obtained experimentally under assayed conditions using the dynamic method: the resulting K_La value, also used in all simulations, being 2.7 h^{-1}.

The three stoichiometric coefficients (g_1, g_2 and c_1), relating to the oxygen balance, plus the nine kinetic constants of the reactions considered in the scheme, are the model parameters to be

Table 1
Kinetics of the proposed model.

Kinetic expression	
$r_1 = k_1 \cdot [Fe^{2+}] \cdot [H_2O_2]$	(1)
$r_2 = k_2 \cdot [Fe^{3+}] \cdot [I]$	(2)
$r_3 = k_3 \cdot [R] \cdot [H_2O_2]$	(3)
$r_4 = k_4 \cdot [R] \cdot [R]$	(4)
$r_5 = k_5 \cdot [M] \cdot [R] \cdot [O_2]$	(5)
$r_6 = k_6 \cdot [M] \cdot [R]$	(6)
$r_7 = k_7 \cdot [MX_1] \cdot [R]$	(7)
$r_8 = k_8 \cdot [MX_1] \cdot [R]$	(8)
$r_9 = k_9 \cdot [MX_2] \cdot [R]$	(9)

Table 2
Mass balances on components model.

Mass balance	
$\frac{d[Fe^{2+}]}{dt} = -r_1 + r_2$	(10)
$\frac{d[Fe^{3+}]}{dt} = r_1 - r_2$	(11)
$\frac{d[H_2O_2]}{dt} = -r_1 - r_3$	(12)
$\frac{d[R]}{dt} = r_1 + r_2 - r_3 - 2 \cdot r_4 - r_5 - r_6 - r_7 - r_8 - r_9$	(13)
$\frac{d[M]}{dt} = -r_5 - r_6$	(14)
$\frac{d[MX_1]}{dt} = r_5 + r_6 - r_7 - r_8$	(15)
$\frac{d[MX_2]}{dt} = r_7 - r_9$	(16)
$\frac{d[O_2]}{dt} = g_1 \cdot r_3 + g_2 \cdot r_4 - c_1 \cdot r_5 + K_L a \cdot (O_2^* - O_2)$	(17)

calibrated from the identification data set—as explained in Section 3.

3. Experimental

3.1. Reagents

High purity acetaminophen (paracetamol) and hydrogen peroxide (30%) were supplied by Sigma–Aldrich. Sulphuric acid (95–97%) was obtained from J.T. Baker and ferrous sulphate (99%) by Fluka. The water used was Milli-Q grade. Pesticides used in this study were commercial formulations of Vydate® (10%, w/v oxamyl, $C_7H_{13}N_3O_3S$), Metomur® (20%, w/v methomyl, $C_5H_{10}N_2O_2S$), Couraze® (20%, w/v imidacloprid, $C_{16}H_{22}ClN_3O$), Perfekthion® (40%, w/v dimethoate, $C_5H_{12}NO_3PS_2$) and Scala® (40%, w/v pyrimethanil, $C_{12}H_{13}N_3$).

3.2. Photochemical reactors

Model-developing experiments were carried out in a plate reactor placed inside a SunTest CPS+ solar box from Atlas with an emission range from 250 to 765 W m^{-2} (complete emission spectrum) using paracetamol aqueous solutions. UV irradiance inside the solar box was measured with a PMA2100 radiometer from Solar Light Company. The plate reactor was connected to a mixing and recirculation tank provided with a sample port as well as pH, temperature, and dissolved oxygen probes. The volume exposed to irradiation was 2 L and the total system volume was 4.5 L—this was so as to maintain the same relationship offered by the CPC pilot plant described elsewhere [26]. Likewise, the optical path length was maintained with a reactor depth of 5 cm, the same diameter as the CPC pilot plant photoreactor. Temperature was kept at 20 °C in all experiments. Data acquisition and pH, temperature and O_2 monitoring (Metler Toledo O_2 4100e) were carried out using DAQ factory software. The pH was adjusted to 2.8 with sulphuric acid before each run. Samples were collected every 5 min for the first 15 min and then every 15 min until the completion of the experiment. Each sample was analysed to determine DOC, iron and H_2O_2 concentrations.

A model testing experiment was carried out with a mixture of five pesticides in a 7 L outdoor pilot plant. The experimental device is a solar detoxification plant with CPC and two absorber tubes with a 50 mm diameter, 46.4 mm internal diameter and 1.5 m length, of which 1.4 m are irradiated. UV radiation is measured by a global UV radiometer (DELTA OHM, model LP UVA 02), mounted on a platform tilted at 37°, which provides data in terms of incident UV (W m^{-2}). The plant was loaded with 7 L of an aqueous solution of the five pesticides, the pH was adjusted to 2.7–2.9 and ferrous iron salt was added. Finally, hydrogen peroxide was added and the CPC uncovered so that the photo-Fenton reaction could begin. Process monitoring and data collection was also conducted via DAQ factory software.

Table 3
Experimental conditions for identification and validation runs.

$[Fe^{2+}]_0$ (mM)	$[H_2O_2]_0$ (mM)	$[TOC]_0$ (mM)	I (W m^{-2})	Use
0.089	35.3	8.33	32	I
0.14	35.3	8.33	32	V
0.178	35.3	8.33	32	I
0.267	35.3	8.33	32	I
0.35	35.3	8.33	32	I
0.44	35.3	8.33	32	I
0.35	8.82	8.33	32	I
0.35	13.23	8.33	32	I
0.35	17.64	8.33	32	V
0.35	26.47	8.33	32	I
0.35	44.1	8.33	32	I
0.35	35.3	4.16	32	I
0.35	35.3	8.33	32	V
0.35	35.3	12.5	32	I
0.35	35.3	16.16	32	I
0.35	35.3	20.83	32	V
0.35	35.3	25	32	I
0.35	35.3	8.33	13	I
0.35	35.3	8.33	19	V
0.35	35.3	8.33	46	I

I: identification; V: validation.

3.3. Analytical methods

During the photo-Fenton treatment, mineralization was followed by TOC determination in a Shimadzu-V_{CHP} TOC analyser and hydrogen peroxide concentration was measured with the ammonium metavanadate colorimetric method. Iron concentration was determined according to the o-phenanthroline standardized spectrometric procedure (ISO 6332).

3.4. Numerical issues

Three optimization procedures were attempted to obtain the model parameters: sequential scanning with a quadratic objective function and preliminary bounds on the constraints (model parameters (k_1–k_9) and (g_1, g_2 and c_1)) conducted in two steps; a Monte Carlo direct search with percentage error as the objective function; and a final fine tune optimization using the MATLAB® optimization toolbox with a weighted quadratic objective function.

In the first step of the sequential scanning procedure, only the hydrogen peroxide consumption profiles were taken into account in the construction of the objective function, so that the kinetic constants of the photo-Fenton cycle could be found. The remaining parameters (kinetic plus stoichiometry constants) were obtained in a second step where the objective function was augmented with a TOC mineralization profile and O_2 evolution. The searching procedure was trapped in local minima for some combinations of kinetic parameters with no improvement of the quadratic objective function defined for the search.

A Monte Carlo method was then implemented for a new parameter adjustment procedure using all the experimental data in the identification set, as referenced in Table 3, and the bound information on the parameters provided by the sequential search. In this way, a random combination of the 12 parameters was used to

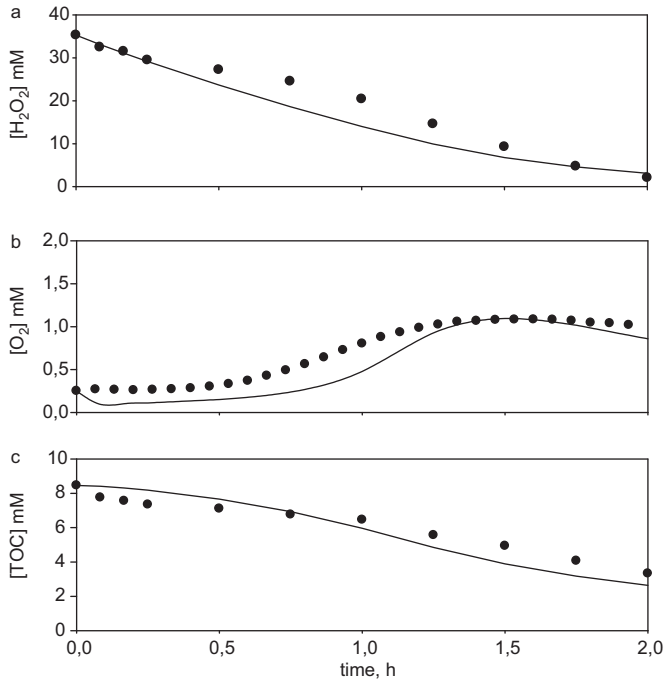

Fig. 2. Experimental and simulated profiles at 0.14 mM Fe^{2+}, 35.3 mM H_2O_2, 8.33 mM TOC and 32 W m^{-2}: (a) H_2O_2, (b) DO and (c) TOC (dots—experimental, lines—model).

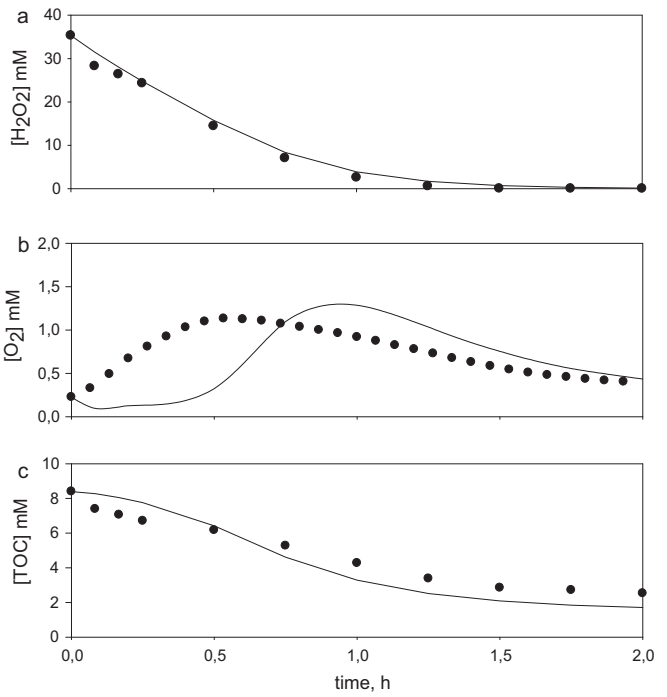

Fig. 3. Experimental and simulated profiles at 0.35 mM Fe^{2+}, 35.3 mM H_2O_2, 8.33 mM TOC and 19 W m^{-2}: (a) H_2O_2, (b) DO and (c) TOC (dots—experimental, lines—model).

simulate the profiles of DO, TOC and H_2O_2 that were compared with the measured ones by the following objective function:

$$J = \sum_{i=1}^{n} i \cdot \left(\sum_{k=1}^{3} abs \left[\frac{X_{kim} - X_{kir}}{X_{kir}} \right] \right) \quad (18)$$

where subscript k stands for the modelled variable (TOC, DO or H_2O_2), subscript m stands for the model value and subscript r stands for the measured value, with n being the number of data points. A weighting function has also been considered to avoid the excessive contribution of the first data points of the series. The absolute value function of the percentage error was selected as the objective function to be minimized in the parameter search. Again, a two-step search was executed—the first, in which the hydrogen peroxide profile as was the unique term in the objective function, as in Eq. (18), and a second step, in which the three terms were in the objective function.

The objective function in the final optimization procedure was defined as follows:

$$\underset{\theta[p_1 \ldots p_{12}]}{J(\theta)} = \sum_{i=1}^{n} \alpha \cdot (H_x(i) - H_s(i))^2 + \beta \cdot (\mathrm{TOC}_x(i) - \mathrm{TOC}_s(i))^2 + \gamma \cdot (\mathrm{DO}_x(i) - \mathrm{DO}_s(i))^2, \quad (19)$$

where the subscript x stands for data and s for simulation. The weighting constants were selected to provide balanced data values. The initial parameter values were taken from the previous Monte Carlo Method implementation results. The non-linear constrained minimization built-in function was used with sequential quadratic programming as the search algorithm. The last procedure was the only one launched when calibrating the model for another pollutant or mixture.

A Monte Carlo procedure was implemented to get an estimation of the model parameters errors by randomly perturbing the experimental observations of the validation data series within the measurements errors. Each perturbed set was fitted via the built-in optimization functions using the already obtained model parameters as initial guesses. The average of the standard deviation obtained for each model parameter and validation data series is given as reliability information on model performance.

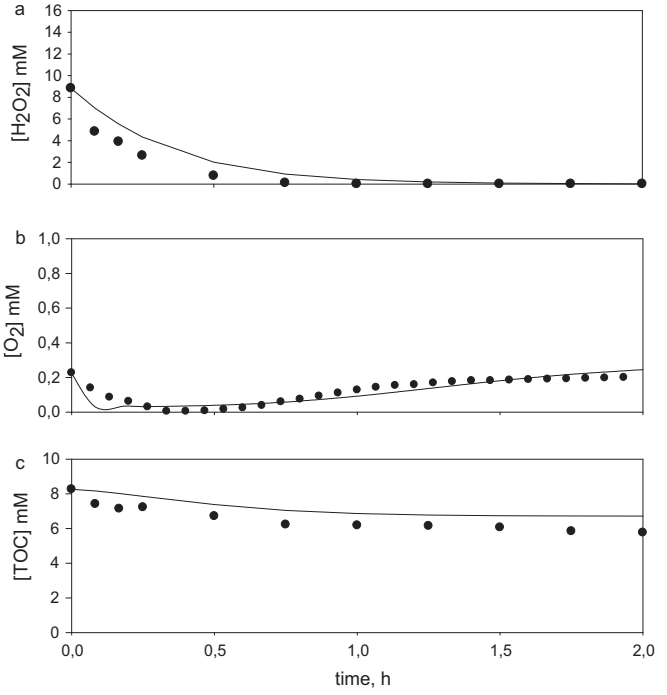

Fig. 4. Experimental and simulated profiles at 0.35 mM Fe^{2+}, 8.83 mM H_2O_2, 8.33 mM TOC and 19 W m^{-2}: (a) H_2O_2, (b) DO and (c) TOC (dots—experimental, lines—model).

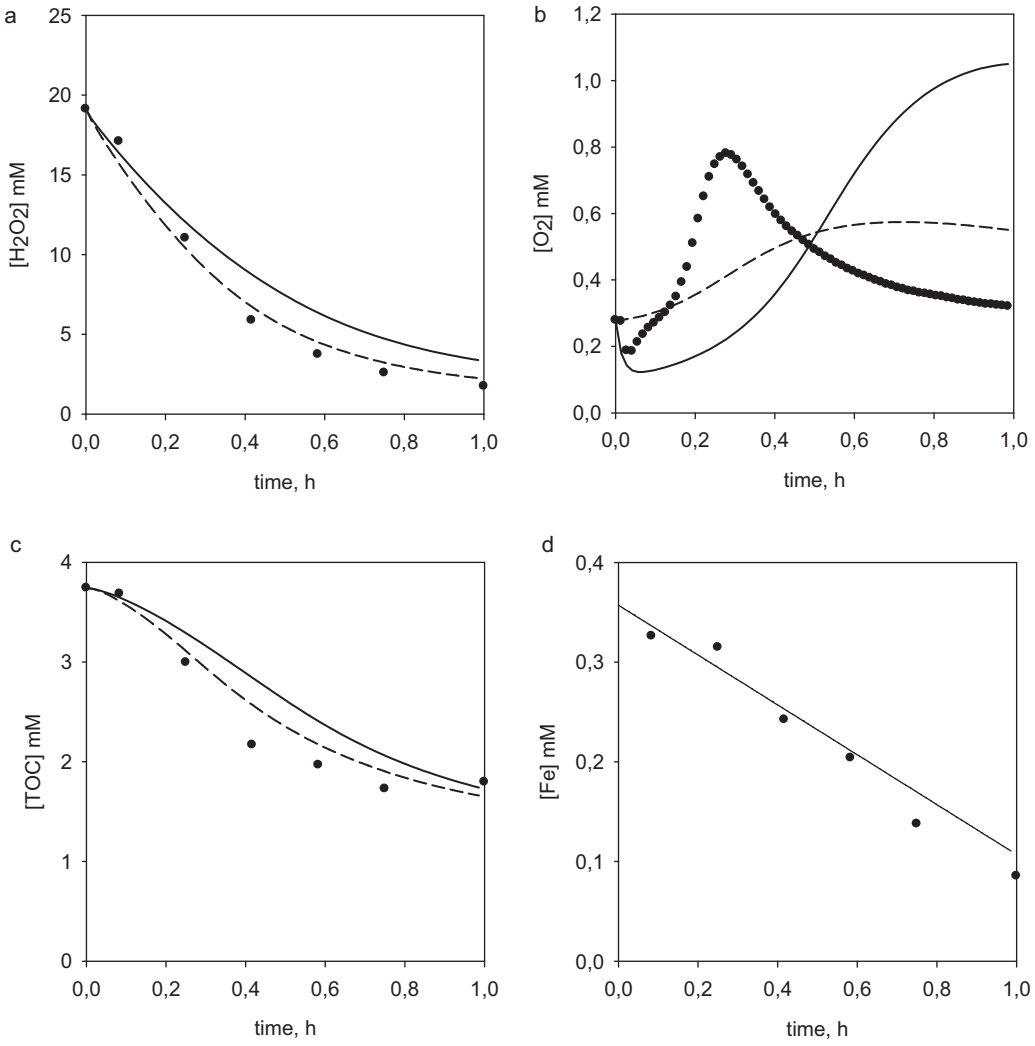

Fig. 5. Profiles for the pilot plant experiment: (a) hydrogen peroxide consumption; (b) dissolved oxygen concentration; (c) TOC removal and (d) total iron concentration. Dots—experimental values; continuous lines—paracetamol calibration; dashed lines—new calibration for pesticide mixture.

4. Results and discussion

In this paper, we have considered an intermediate solution to represent the kinetics of the photo-Fenton mineralization process whilst presenting a model with only a few simple steps corresponding to the group reactions architecture cited by Kang et al. above. No enhancement of the photo-Fenton cycle is considered by interactions of intermediates and Fe states, and a profound influence in overall process is given to the inorganic reaction group, especially to the O_2-involved reactions. Another distinguishing feature is the lumped state for radical species, which is differentiated by the works considering first-principles-related modelling. On the other hand, the need for TOC fractionation has been considered and is also the scheme followed here. The structure of this fractionation, that is, the number of lumped species which share similar oxidation reactivity, is a key element in the model. So, the proposed model has been compared with other structures using the parsimony principle, which should always be considered in model development. Inclusion of five oxidized intermediates did not improve the prediction capabilities of the model and would increase the number of parameters to be estimated from regression data. Stoichiometry of the single step considered is the other subject containing uncertainty. In fact, this may vary both with operating conditions and with the chemical nature of the treated contaminant. In some cases the Fe concentration acts as a reactant (and is consumed in the subsequent redox cycles) or acts as a nearly ideal catalyst—meaning only a minimum starting level is necessary to drive the process. Strong pH dependence is usually reported for Fe speciation, and the ratio to hydrogen peroxide is also a determinant condition for this behaviour. Stoichiometry coefficients have also been considered as model parameters and these appear in the final form of the model.

Table 4 shows the final result of the parameter search and Figs. 2–4 compare the experimental and simulated profiles as example of model performance.

Some points are remarkable with regard to the values obtained in Table 4. First, the highest kinetic constant value corresponds to reaction (4) between inorganic radicals, as is also the case for the references in literature for models describing a detailed inorganic chemistry [14,15]. In fact, these papers report a value close to $10^9\ M^{-1}\ s^{-1}$ for the reaction of two hydroxyl radicals and their citations pointed to the same source work for collecting kinetic data [27]. Thus, k_4 given in Table 4 should be taken as a coherent value. The controlling steps of the process are the reactions involved in the photo-Fenton cycle, as shown by the lowest k values given by the searching procedure. The literature values for the thermal Fenton cycle reaction steps are $63\ M^{-1}\ s^{-1}$ and $0.002\ M^{-1}\ s^{-1}$ for Fe^{2+} and Fe^{3+} reacting with hydrogen peroxide, respectively. The enhancement effect due to UV light raises the second value giving a three-orders-of-magnitude ratio between the two steps. In this

Table 4
Model calibration results.

Kinetic constants ($mM^{-1}\,h^{-1}$)									Stoichiometric coefficients		
k_1	k_2	k_3	k_4	k_5	k_6	k_7	k_8	k_9	g_1	g_2	c_1
8.81 ± 0.7	5.63 ± 0.9	75.8 ± 11	42,798 ± 5	2643 ± 20	257 ± 40	2865 ± 33	271 ± 30	107 ± 11	0.75 ± 0.16	0.47 ± 0.07	0.10 ± 0.04

case, considering the explicit UV light value in the kinetic expression, a ratio of two orders of magnitude results, which is consistent with the literature data. The kinetic constant of the organic matter oxidation step with an oxygen presence corresponding to reaction (5) is also higher than the oxidation of reaction (6), by radicals alone, as has been observed experimentally. And the final mineralization steps report kinetic values lower than those for oxidation, also a fact that has been evidenced. On the other hand, the significance of the stoichiometry coefficients might be attributable to the chemical nature of the compound.

As can be seen in Figs. 2–4 the model gives a good prediction of the hydrogen peroxide and TOC profiles at the conditions tested. The model is able to predict the maximum O_2 evolution, which is an interesting feature of the photo-Fenton process, as it is the reaction time at which the maximum availability of radical species is found. Fig. 2 shows the model performance when initial concentration of Fe^{2+} (0.14 mM) is lower than that of the most applied operating conditions (0.35 mM Fe^{2+}, 35.3 mM H_2O_2, 8.33 mM TOC and 32 W m^{-2}). Fig. 3 presents the variable profiles at an irradiance of 19 W m^{-2} which is the average annual UV radiation in Almería (Spain). Finally, a case of low dosage of hydrogen peroxide (8.82 mM) is depicted in Fig. 4.

Dissolved oxygen curve of the model presents a low delay with regard to experimental points at 19 W m^{-2} irradiance, although the estimated maximum value is close to the experimental observation. At limiting H_2O_2 conditions, dissolved oxygen is consumed and organic carbon mineralization is stopped. The proposed model adequately predicts these observed phenomena as shown in Fig. 4.

The applicability of the proposed model was tested at outdoor pilot plant scale. An aqueous solution of a mixture of five commercial pesticides with an initial TOC of 4 mM was used to check operational conditions closely related to real toxic wastewater treatment. Fig. 5 presents the results of this experiment. Due to the narrow variation observed in temperature and irradiance levels during the experimental time, average values of 30 °C and 17 W m^{-2} have been considered for temperature and irradiance, respectively. The gas–liquid mass transfer coefficient for O_2, obtained by the dynamic method, for this plant was 0.84 h^{-1}. A constant loss of Fe by precipitation occurred during the assay, and this fact was taken into account by an additional term in the mass balance equations corresponding to the Fe states. As can be seen in Fig. 5d, the change in total Fe, due to this phenomenon is adequately represented by the model.

What is also remarkable is the closeness of the simulated profiles of hydrogen peroxide consumption and TOC mineralization to the measured data when the simulation is conducted with the parameters presented in Table 4—that is, calibrated with paracetamol as a model pollutant. One possible reason for this result might be that the structure of the proposed model possesses a great enough degree of freedom to gather the information in the data. Besides, the hydrogen peroxide reactivity is strongly determined by the initial conditions of catalyst, UV light availability, the ratio reactant/catalyst; and the initial TOC concentration—rather than the chemical nature of organic matter or the number of species present.

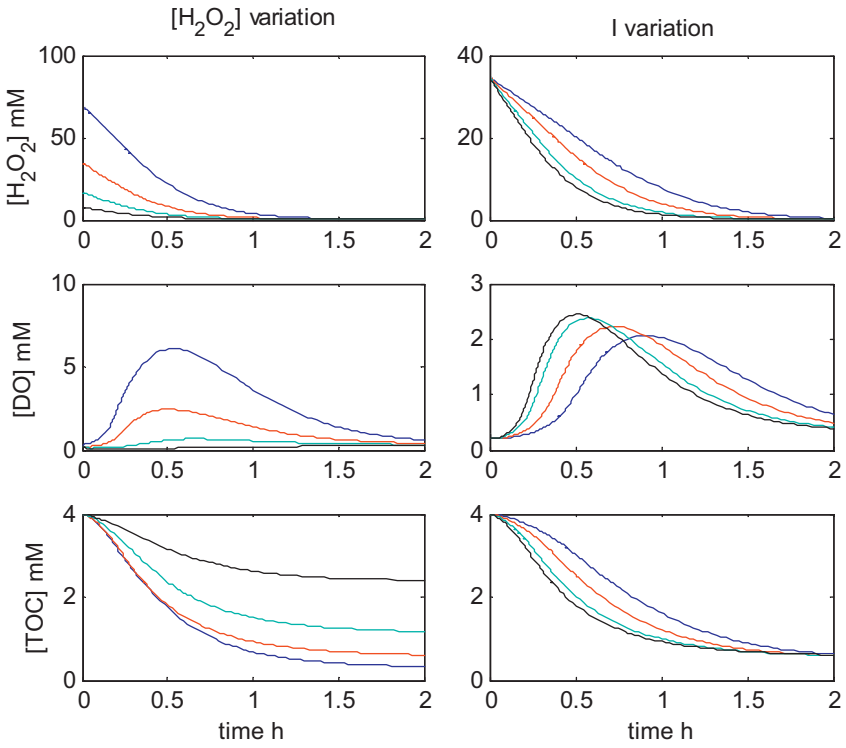

Fig. 6. Simulation studies on photo-Fenton profiles for (a) hydrogen peroxide concentration, (b) DO_2 evolution and (c) TOC removal, conducted at varying irradiance levels (left side) and initial hydrogen peroxide (right side).

Regarding the O_2 evolution, in Fig. 5b, the model fails in predicting the maximum peak, which is over-predicted and delayed. In this case, the chemical properties of the organic matter – with completely different fractionation in terms of intermediates reactivity when compared to the paracetamol study – might be the reason for the discrepancy. The average oxidation state for paracetamol is −0.18 whilst for the pesticide mixture it is −0.25. In fact, the improved fitted response when the model is recalibrated by the procedure described in Section 3.4 still shows the same behaviour. Nonetheless, the model has shown the main experimental facts of the photo-Fenton process within the range of the variables studied.

For simulation purposes, the model shows the behaviour of a photo-Fenton plant at varying environmental or operational conditions. For instance, Fig. 6 illustrates the variations in the profiles discussed above for changes in the irradiance levels (environmental variable) and the initial hydrogen peroxide concentration (operational variable) at a fixed TOC and initial catalysts load. Trends in the process behaviour are indicated by the proposed model as can be seen in Fig. 6. Inadequate dosage ratio leads to reactant waste as pointed out by the high O_2 production rate, even with the over-predicted value shown in Fig. 6. A lower dosage of hydrogen peroxide should be used to operate the photo-Fenton process efficiently. The use of insufficient reactant to attack a given TOC concentration is also reflected by tracking the O_2 profile, which shows a flat or diminishing evolution when this is the case. A lower spread is observed in the O_2 profiles when irradiance effects are considered for a fixed reactant/TOC ratio with a displacement of the O_2 peak location occurring earlier the higher the irradiance, but with similar magnitude. The reactivity enhancement of the system as a result of increasing irradiance is clearly shown by the more pronounced decrease in hydrogen peroxide concentration. On the other hand, an equal value of final TOC with different irradiance is predicted, showing the advantage of stopping the process at a predetermined time covering the TOC specification for a potential coupling with another treatment.

Efforts to develop models capturing the principal process features complemented by the online instrumentation would result in an adequate tool for controlling and operating a photo-Fenton-based plant efficiently. Experience of this can be found in Alvarez et al., where a solar pilot plant was the experimental device tested to identify a model for peroxide concentration evolution as a function of sampled data for iron level, online UV radiation and percentage frequency range for the H_2O_2 pump [28]. A second order plus delay transfer function was obtained by pulse input excitation and the standard modes of PID control were tested. Furthermore, recent advances in wastewater monitoring, such as a paracetamol-sensing device, developed by Quintino de Oliveira et al., would facilitate the operation of this wastewater technology [29].

5. Conclusions

Variation in dissolved oxygen concentration due to changes in the photo-Fenton process reaction conditions has been reported as an indicator for the efficient use of hydrogen peroxide. A semi-empirical model has been developed to predict not only TOC mineralization and hydrogen peroxide consumption but also dissolved oxygen concentration. The model structure is based on a group of reactions so that the total number of parameters is assumable and light intensity is considered explicitly within the model.

The model was calibrated and validated using paracetamol solutions as the model pollutant, obtaining a good prediction of the hydrogen peroxide and TOC profiles under the conditions tested. Around the most applied or most similar conditions, the model was able to predict O_2 evolution—whilst under extreme conditions; the model was only able to predict the O_2 curve maximum.

The applicability of the proposed model was also tested at outdoor pilot plant scale for an aqueous solution of a mixture of five commercial pesticides. Results showed good predictions for TOC mineralization and hydrogen peroxide consumption. Refinements are needed for O_2 predictions, given that this profile is strongly determined by the nature and the number of chemicals reacting.

For simulation purposes, the model is capable of showing the behaviour of a photo-Fenton treatment plant when varying environmental or operational conditions (such as light intensity) depending on plant location and/or season as well as hydrogen peroxide concentration. The mineralization level for a given treatment time can be predicted when different irradiances are involved in the process, which is dependent on plant location. Additionally, hydrogen peroxide dosage can be optimized at varying iron concentrations.

Acknowledgements

L. Santos-Juanes wants to acknowledge Ministerio de Ciencia e Innovación for his Juan de la Cierva scholarship. This research was funded by the Ministerio de Ciencia e Innovación (Spanish Ministry of Science and Innovation) (CTQ2010-20740-C03-01), the European Regional Development Fund (ERDF) and by the Consejería de Innovación, Ciencia y Empresa de la Junta de Andalucía (Andalusian Regional Government) (FOTOMEM, project, P08-RNM-03772).

References

[1] E. Elmolla, C. Malay, J. Hazard. Mater. 192 (2011) 1418–1426.
[2] M. Klavarioti, D. Mantzavinos, D. Kassinos, Environ. Int. 35 (2009) 402–417.
[3] S. Navalon, M. Alvaro, H. Garcia, Appl. Catal. B 99 (2010) 1–26.
[4] B. Ahmed, E. Limem, A. Abdel-Wahab, B. Nasr, Ind. Eng. Chem. Res. 50 (2011) 6673–6680.
[5] A. Zapata, I. Oller, L. Rizzo, S. Hilgert, M.I. Maldonado, J.A. Sánchez-Pérez, S. Malato, Appl. Catal. B 97 (2010) 292–298.
[6] J. Soler, L. Santos-Juanes, P. Miró, R. Vicente, A. Arques, A.M. Amat, J. Hazard. Mater. 188 (2011) 181–187.
[7] L. Santos-Juanes Jordá, M.M. Ballesteros Martín, E. Ortega Gómez, A. Cabrera Reina, I.M. Román Sánchez, J.L. Casas López, J.A. Sánchez Pérez, J. Hazard. Mater. 186 (2011) 1924–1929.
[8] F.J. Beltrán, A. Aguinaco, J.F. García-Araya, Appl. Catal. B 100 (2010) 289–298.
[9] G. Li Puma, V. Puddu, H.K. Tsang, A. Gora, B. Toepfer, Appl. Catal. B 99 (2010) 388–397.
[10] A.Y. Sychev, V.G. Isak, Russ. Chem. Rev. 64 (1995) 1105–1129.
[11] J.J. Pignatello, E. Oliveros, A. MacKay, Crit. Rev. Environ. Sci. Technol. 36 (2006) 1–84.
[12] S. Pang, J. Jiang, J. Ma, Environ. Sci. Technol. 45 (2011) 307–312.
[13] N. Kang, S.L. Dong, Y. Jeyong, Chemosphere 47 (2002) 915–924.
[14] H. Kusic, N. Koprivanac, A. Loncaric, I. Selanec, J. Hazard. Mater. 136 (2006) 632–644.
[15] G. Ortiz de la Plata, O. Alfano, A. Cassano, Appl. Catal. B 95 (2010) 14–25.
[16] M. Pérez-Moya, M. Graells, P. Buenestado, H.D. Mansilla, Appl. Catal. B 84 (2008) 313–323.
[17] M. Pérez-Moya, H.D. Mansilla, M. Graells, J. Chem. Technol. Biotechnol. 86 (2011) 826–831.
[18] S.M. Alpert, D.R.U. Knappe, J.J. Ducoste, Water Res. 44 (2010) 1797–1808.
[19] M. Mohajerani, M. Mehrvar, F. Ein-Mozaffari, Can. J. Chem. Eng. 9999 (2011) 1–11.
[20] L. Santos-Juanes, J.L. García Sánchez, J.L. Casas López, I. Oller, S. Malato, J.A. Sánchez Pérez, Appl. Catal. B 104 (2011) 316–323.
[21] D. Vogna, R. Marotta, A. Napolitano, M. d'Ischia, J. Org. Chem. 67 (2002) 6143–6151.
[22] R. Andreozzi, V. Caprio, R. Marotta, D. Vogna, Water Res. 37 (2003) 993–1004.
[23] J. Radjenovic, C. Sirtori, M. Petrovic, D. Barcelo, S. Malato, Appl. Catal. B 89 (2009) 255–264.
[24] M. Skoumal, P.L. Cabot, F. Centellas, C. Arias, R.M. Rodriguez, J.A. Garrido, E. Brillas, Appl. Catal. B 66 (2006) 228–240.
[25] L. Yang, L.E. Yu, M.B. Ray, Water Res. 42 (2008) 3480–3488.
[26] M.M. Ballesteros Martín, J.A. Sánchez Pérez, J.L. García Sánchez, J.L. Casas López, S. Malato Rodríguez, Water Res. 43 (2009) 3838–3848.
[27] G.V. Buxton, C.L. Greenstock, W.P. Helman, A.B. Ross, J. Phys. Chem. Ref. Data 17 (1988) 513–886.
[28] J.D. Alvarez, W. Gernjak, S. Malato, M. Berenguel, M. Fuerhacker, L.J. Yebra, J. Sol. Energy Eng. 129 (2007) 37–44.
[29] M.C. Quintino de Oliveira, M.R. de Vasconcelos Lanza, J.L. Paz Jara, M.P. Taboada Sotomayor, Int. J. Electrochem. (2011) 1–11.